Metal-Cation-Mediated Hydrolysis of Phosphonoformate Diesters: Chemoselectivity and Catalysis[1]

Robert A. Moss,* Hugo Morales-Rojas,[†] Saketh Vijayaraghavan, and Jingzhi Tian

Contribution from the Department of Chemistry and Chemical Biology, Rutgers, The State University of New Jersey, New Brunswick, New Jersey 08903

Received July 18, 2003; E-mail: moss@rutchem.rutgers.edu

Abstract: Hydrolyses in D$_2$O (pD 1.7–3.1) of dimethyl (**7**), methyl phenyl (**8**), phenyl methyl (**9**), and diphenyl (**10**) phosphonoformate diesters are substantially accelerated by Ce(IV), Th(IV), Zr(IV), and Hf(IV) cations. Chemoselectivity is observed, whereby Zr(IV) and Hf(IV) principally direct P−OR hydrolysis, whereas Th-(IV) and Ce(IV) mainly direct C−OR hydrolysis. Leaving group efficiency (OMe vs OPh) modulates the chemoselectivity. The metal cations also mediate further hydrolytic reactions of the initially produced phosphonoformate monoesters **14**, **15**, **18**, and **20**. The origins of the P−OR/C−OR selectivity are discussed in terms of the metal cation hydroxo species likely to be present in solution and the kinetics of the reactions.

The phosphonoformate trianion ("foscarnet"), **1** (PFA), is active against herpes simplex virus and AIDS-related human cytomegalovirus.[2] However, PFA is largely trianionic at physiological pH[3] and displays poor membrane permeability and low bioavailability. Interest therefore focuses on PFA mono-, di-, and triesters as PFA prodrugs.[4−6] For example, *P*-monoesters are more easily biotransformed to PFA than *C*-monoesters, and aryl *P*-monoesters are more active than their alkyl analogues.[4] Additionally, the activities of PFA triesters **2**, bearing an aromatic *P*-ester residue, and the corresponding monoanionic PFA diesters **3** were similar, suggesting that the aryl residue is selectively hydrolyzed to the corresponding diester.[4] Mechanistic
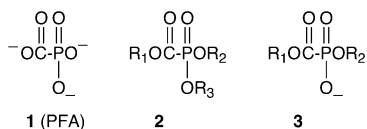
studies of PFA solvolysis have appeared.[5c,d,6] Of special interest is the observation that PFA triesters are orders of magnitude more reactive at P than simple phosphonate diesters due to the electronic influence of the α-carbonyl group.[5c,e]

We, and others,[5a,7] have been interested in PFA diesters **3** as PFA prodrugs. The diesters are relatively stable toward hydrolysis in neutral and mildly acidic aqueous solutions, whereas triesters **2** are more labile and can also suffer P−C backbone cleavage. Representative of the diesters, diethyl phosphonoformate (**3**, R$_1$ = R$_2$ = Et) cleaves in pH 7.0 Tris buffer with k_{obs} = 5 × 10^{-8} s^{-1} ($t_{1/2} \approx$ 160 d),[5b] whereas base catalyzed hydrolysis occurs more rapidly (by C−O cleavage) to yield *P*-monoesters **4**, which can be further hydrolyzed to PFA; eq 1.
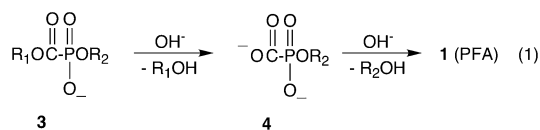
In a seminal and stimulating study, Thatcher and Ferguson reported that aminocyclodextrins accelerated the aminolysis, esterolysis, and hydrolysis of *C*-phenyl PFA diesters (**3**, R$_1$ = Ph).[5b] Hydrophobic bonding of the phenyl moiety inside the (α or β) cyclodextrin cavity and electrostatic interactions of the phosphate group with the positively charged ammonium groups on the rim of the torus contributed to the observed reactivity.[5b]

Our interest in PFA diester hydrolysis derives from previous studies of metal-cation-mediated scission of phosphate diesters and phosphonate monoesters. Ce(IV), Th(IV), Zr(IV), and Hf-(IV) salts in aqueous solution manifest high reactivity in the hydrolysis of both activated and unactivated phosphate diesters.[8] Soluble forms of Ce^{4+} and Th^{4+} afford accelerations of ∼2.4−2.8 billion in the hydrolysis of bis-*p*-nitrophenyl phosphate.[8,9] More remarkably, an acidic aqueous solution of uncomplexed

† Current address: Centro de Investigaciones Quimicas, Universidad Autonoma del Estado de Morelos, Cuernavaca, Morelos, Mexico.
(1) Taken in part from the Ph.D. dissertations of H.M.-R., S. V. Rutgers University, New Brunswick, NJ, 2001 and 2002, respectively.
(2) *Physicians Desk Reference*; Medical Economics Co.: Montvale, NJ, 2000; pp 600−603. See also: Obert, B. *Pharmacol. Ther.* **1989**, *40*, 213.
(3) The pK_a values of PFA at μ = 0.1 are 0.78, 3.61, and 7.57: Song, B.; Chen, D.; Bastian, M.; Martin, R. B.; Sigel, H. *Helv. Chim. Acta* **1994**, *77*, 1738.
(4) Noren, J. O.; Helgstrand, E.; Johansson, N. G.; Misiorny, A.; Stening, G. *J. Med. Chem.* **1983**, *26*, 264.
(5) (a) Ferguson, C. G.; Gorin, B. I.; Thatcher, G. R. J. *J. Org. Chem.* **2000**, *65*, 1218. (b) Ferguson, C. G.; Thatcher, G. R. J. *Org. Lett.* **1999**, *1*, 829. (c) Krol, E. S.; Thatcher, G. R. J. *J. Chem. Soc., Perkin Trans. 2* **1993**, 793. (d) Krol, E. S.; Davis, J. M.; Thatcher, G. R. J. *Chem. Commun.* **1991**, 118. (e) Thatcher, G. R. J.; Krol, E. S.; Cameron, D. R. *J. Chem. Soc., Perkin Trans. 2* **1994**, 683.
(6) (a) Mitchell, A. G.; Nicholls, D.; Irwin, W. J.; Freeman, S. *J. Chem. Soc., Perkin Trans. 2* **1992**, 1145. (b) Mitchell, A. G.; Nicholls, D.; Walker, I.; Irwin, W. J. Freeman, S. *J. Chem. Soc., Perkin Trans. 2* **1991**, 1297.

(7) Gorin, B. I.; Ferguson, C. G.; Thatcher, G. R. J. *Tetrahedron Lett.* **1997**, *38*, 2791.
(8) Bracken, K.; Moss, R. A.; Ragunathan, K. G. *J. Am. Chem. Soc.* **1997**, *119*, 9323.
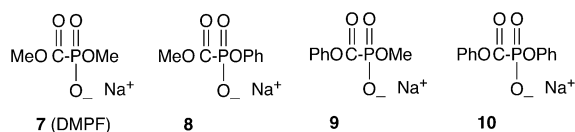(9) Moss, R. A.; Zhang, J.; Bracken, K. *Chem. Commun.* **1997**, 1639.

Ce^{4+} hydrolyzes dimethyl phosphate (**5**, DMP) with an acceleration of ~2×10^8, reducing its half-life from >8000 years at pH 7 to only 22 min.[10] Subsequent H$_2$^{18}O labeling studies

$$\underset{\textbf{5}}{MeOPOMe} \qquad \underset{\textbf{6}}{MePOPNP}$$
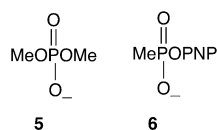
revealed that Ce^{4+}-mediated hydrolysis of DMP occurs with 91% P–O cleavage and about 9% O–Me cleavage.[11] The resemblance between DMP and dimethyl phosphonoformate (**3**, R$_1$=R$_2$=Me, DMPF) is both clear and suggestive. Zr^{4+} and Hf^{4+} are also active in the mediated hydrolysis of phosphate diesters,[12] while Ce^{4+}, Th^{4+}, and Zr^{4+} display huge kinetic advantages in the cleavage of *p*-nitrophenyl methylphosphonate, **6**.[13]

Our studies of metal-mediated phosphorolysis appeared within a matrix of many related contributions.[14] With respect to DMP,[10,11] for example, Co(III)-cyclen,[15] and Cp$_2$MoCl$_2$[16] have also been shown to educe very large hydrolytic rate accelerations. And the hydrolyses of more reactive phosphodiesters are speeded by a variety of highly charged metal cations.[17]
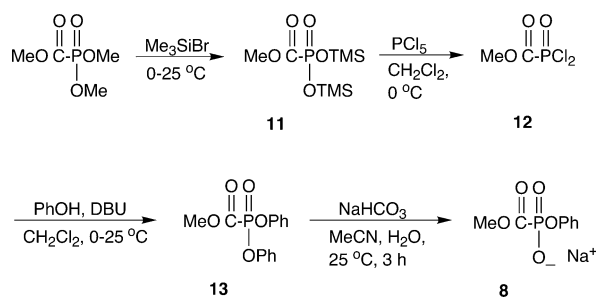
Given the strong catalysis exhibited by metal cations in phosphodiester hydrolysis, we examined the reactivity of Ce-(IV), Th(IV), Zr(IV), and Hf(IV) toward DMPF, **7** (i.e., **3** with R$_1$ = R$_2$ = Me).[18] Our principal finding was an unprecedented

$$\underset{\textbf{7 (DMPF)}}{MeO\,C\text{-}POMe} \qquad \underset{\textbf{8}}{MeO\,C\text{-}POPh} \qquad \underset{\textbf{9}}{PhO\,C\text{-}POMe} \qquad \underset{\textbf{10}}{PhO\,C\text{-}POPh}$$

chemoselectivity in which acidic aqueous solutions of Ce^{4+} and Th^{4+} directed the C–OMe hydrolysis of DMPF, whereas Zr^{4+} and Hf^{4+} afforded preferential P–OMe hydrolysis.[18] All the hydrolyses were accelerated, relative to simple acidic catalysis. The origins of the accelerations and chemoselectivity were ascribed to the nature of the M^{4+}–DMPF interactions and the aggregation states of M^{4+} in aqueous solutions.[18]

In this full paper, we extend our studies of metal-cation-mediated hydrolysis to phosphonoformates **8–10**, in which the Me esters of **7** are systematically replaced by the more hydrolytically sensitive Ph esters. An underlying question is how robust is the P–OR > C–OR chemoselectivity exhibited by Zr^{4+} and Hf^{4+} toward phosphonoformate diesters? For instance, does the kinetically controlled P–OR > C–OR discrimination

(10) Moss, R. A.; Ragunathan, K. G. *Chem. Commun.* **1998**, 1871.
(11) Moss, R. A.; Morales-Rojas, H. *Org. Lett.* **1999**, *1*, 1791.
(12) Moss, R. A.; Zhang, J.; Ragunathan, K. *Tetrahedron Lett.* **1998**, *39*, 1529.
(13) Moss, R. A.; Ragunathan, K. G. *Langmuir* **1999**, *15*, 107.
(14) For "early" studies, see: (a) Breslow, R.; Huang, D. L. *Proc. Natl. Acad. Sci. U.S.A.* **1991**, *88*, 4080. (b) Morrow, J. R.; Buttrey, L. A.; Shelton, V. M.; Berback, K. A. *J. Am. Chem. Soc.* **1992**, *114*, 1903. (c) Morrow, J. R.; Buttrey, L. A.; Berback, K. A. *Inorg. Chem.* **1992**, *31*, 16. (d) Komiyama, M.; Matsumura, K.; Matsumoto, Y. *Chem. Commun.* **1992**, 640. (e) Schneider, H.-J.; Rammo, J.; Hettich, R. *Angew. Chem., Int. Ed. Engl.* **1993**, *32*, 1716. (f) Rammo, J.; Schneider, H.-J. *Liebigs Ann.* **1996**, 1757. (g) Takasaki, B. K.; Chin, J. *J. Am. Chem. Soc.* **1993**, *115*, 9337. (h) Breslow, R.; Zhang, B. *J. Am. Chem. Soc.* **1994**, *116*, 7893.
(15) Kim, J. H.; Chin, J. *J. Am. Chem. Soc.* **1992**, *114*, 9792.
(16) Kuo, L. Y.; Barnes, L. A. *Inorg. Chem.* **1999**, *38*, 814.
(17) (a) Williams, N. H.; Takasaki, B.; Wall, M.; Chin, J. *Acc. Chem. Res.* **1999**, *32*, 485. (b) Blasko, A.; Bruice, T. C. *Acc. Chem. Res.* **1999**, *32*, 475. (c) Krämer, R. *Coord. Chem. Rev.* **1999**, *182*, 243. (d) Roigk, A.; Hettich, R.; Schneider, H.-J. *Inorg. Chem.* **1998**, *37*, 751. (e) Molenveld, P.; Engbersen, J. F. J.; Reinhoudt, D. N. *Chem. Soc. Rev.* **2000**, *29*, 75.
(18) Moss, R. A.; Morales-Rojas, H. *J. Am. Chem. Soc.* **2001**, *123*, 7457.

Scheme 1

survive with substrate **9**, where the "dice are loaded" in favor of C–O cleavage? We also revisit the question of the aggregation states of the chemoselective M^{4+} catalysts.

Results

Synthesis. The sodium salt of DMPF (**7**) was prepared by sodium iodide demethylation[4] of commercial trimethyl phosphonoformate (**2**, R$_1$ = R$_2$ = R$_3$ = Me) in refluxing acetone. It was characterized by ^{1}H and ^{31}P NMR spectroscopy, as well as elemental analysis.
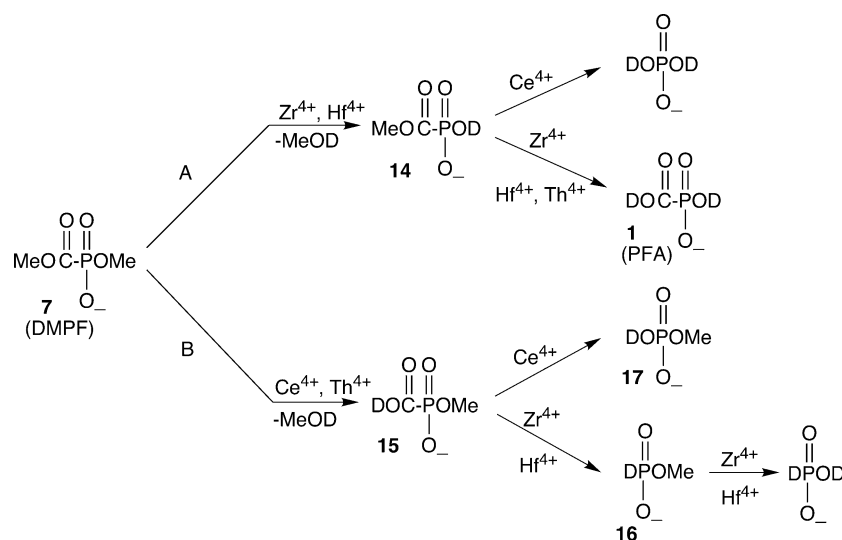
Substrate **8** was prepared by the more complicated sequence of Scheme 1. Trimethyl phosphonoformate was converted in 91% yield to *P*-bis-trimethylsilyl *C*-methyl phosphonoformate (**11**) with trimethylsilyl bromide. Treatment of the latter with PCl$_5$ gave 69% of the phosphonodichloridate **12**, which, upon reaction with phenol and DBU in CH$_2$Cl$_2$, afforded *C*-methyl diphenyl phosphonoformate **13**. Hydrolysis of **13** with dilute base gave the desired *C*-methyl *P*-phenyl phosphonoformate **8**, in 60% yield for the last two steps. Substrate **8** was characterized by ^{1}H and ^{31}P NMR and by elemental analysis. It has been previously prepared by Noren using a less accessible procedure.[4]

Substrate **9** was made by reacting phenyl chloroformate with trimethyl phosphate to yield *C*-phenyl dimethyl phosphonoformate (**2**, R$_1$ = Ph, R$_2$ = R$_3$ = Me) in 97% yield, followed by sodium iodide demethylation of the latter in refluxing acetone (80%). Phenyl methyl phosphonoformate was fully characterized.

Finally, diphenyl phosphonoformate (**10**) was prepared by conversion of diphenyl *H*-phosphite [(PhO)$_2$PH] to the *P*-anion with NaH in THF, followed by reaction of the latter with phenyl chloroformate to give triphenyl phosphonoformate (**2**, R$_1$ = R$_2$ = R$_3$ = Ph). This was directly hydrolyzed to **10** by sodium bicarbonate in aqueous acetonitrile. Substrate **10** was purified by column chromatography and fully characterized (as the hemihydrate).

Reactions and Kinetics; DMPF. We first examined the hydrolysis of DMPF (**7**), mediated by Ce^{4+}, Th^{4+}, Zr^{4+}, and Hf^{4+}.[18] Reactions were initiated by mixing 10 mM of DMPF with 25 mM ZrCl$_4$, HfCl$_4$, Ce(NH$_3$)$_2$(NO$_3$)$_6$, or Th(NO$_3$)$_4$·4H$_2$O at 25 °C in D$_2$O containing 0.5 M NaClO$_4$. Pyrazine was added as an internal ^{1}H NMR integration standard; *O*-methyl methylphosphonate served a similar purpose for ^{31}P NMR spectroscopy. The pD's of the unbuffered reaction solutions were established by hydrolysis of the metal cations: Zr^{4+}, 1.7; Hf^{4+}, 2.2; Ce^{4+}, 1.9; Th^{4+}, 3.1. The reactions were followed by ^{1}H and ^{31}P NMR, and products were verified by NMR spiking experiments with authentic materials (see Experimental Section). For ^{31}P NMR experiments, it was necessary to remove the metal

Scheme 2[a]

[a] Species are depicted in anticipated ionization states in D$_2$O at experimental pD's.

cations by chelation with EDTA or tartrate in order to suppress line broadening. Reaction aliquots, so treated, were then examined at appropriate time intervals.

Under the foregoing conditions, Zr^{4+}- or Hf^{4+}-mediated hydrolyses of DMPF occur mainly at P−OMe. Thus, the proton NMR spectrum of DMPF in D$_2$O shows Me signals at δ 3.71 (s, C−OMe) and 3.58 (d, J_{P-H} = 11.1 Hz, P−OMe). Reaction with, e.g., Hf^{4+}, mainly removes the P−OMe *doublet*. In its place, *singlets* appear at δ 3.33 (MeOD) and 3.79 for the product *C*-monoester **14**. Similar changes attend the reaction of DMPF
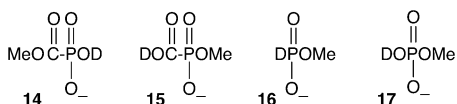
with Zr^{4+}. A minor competitive pathway, in each case, involves C−OMe cleavage to *P*-monoester **15**. Here, the *C*-OMe singlet of DMPF is reduced, and the *P*-OMe doublet of **15** appears at δ 3.74 (J_{P-H} = 11.7 Hz); see Scheme 2.

The **14/15** distributions of the Hf^{4+} and Zr^{4+} cleavages of DMPF were best ascertained by ^{31}P NMR spectroscopy of EDTA-quenched reaction aliquots taken at 15, 30, or 60 min. The ^{1}H-decoupled ^{31}P NMR resonances of DMPF, **14**, and **15** in D$_2$O appeared at δ −2.5, −5.2, and 6.9, respectively.[19] Integration gave the **14/15** distributions ($\pm$2%) as 79:21 from Zr^{4+} and 90:10 from Hf^{4+}; cf. Table 1.[20] The **14/15** distribution for the Zr^{4+} cleavage of DMPF was similarly determined by ^{31}P NMR in H$_2$O (locked to D$_2$O in a capillary tube). After integration of the appropriate signals, the distribution was 80:20, experimentally identical to the cleavage distribution found in D$_2$O.

The reaction kinetics were followed by monitoring MeOD formation in the proton NMR. Pseudo-first-order behavior was

(19) The ^{31}P NMR chemical shifts vary somewhat in the presence of the different metal cations. They are also sensitive to pD or pH.

(20) A labeling experiment was conducted in 47% ^{18}O−H$_2$O with DMPF (P−O^{13}CH$_3$) and Hf(IV). ^{31}P and ^{1}H NMR monitoring showed the formation of **14**, with stoichiometric ^{18}O incorporation, and released ^{13}CH$_3^{16}$OH (only). Therefore, P−O−Me scission of DMPF by Hf(IV) and (presumably) Zr-(IV) occurred only by P−O cleavage.

Table 1. Kinetic Data for Dimethyl Phosphonoformate (**7**) and **14**[a]

	10^4 k_{obs}[b] (s^{-1})			product distributions for cleavage of **7** (%)[c]	
M(IV)	DMPF (**7**)	**14**	$k_{M(IV)}/k_{D+}$[d]	**14**	**15**
Zr	4.4	0.022	3300	79	21
Hf	4.0	0.026	3100	90	10
Th	1.3	0.42	980		>95
Ce	5.2[e]	0.93[e]	3900	10	90

[a] Conditions [M(IV)] = 25 mM, [substrate] = 10 mM, 0.5 M NaClO$_4$ in D$_2$O, 25 °C, pD 1.7 (Zr), 2.2 (Hf), 3.1 (Th), 1.9 (Ce). [b] Monitored by ^{1}H NMR integration of released MeOD relative to an internal pyrazine standard. Errors of duplicate runs $\pm$ 8% (maximum). [c] From ^{31}P NMR spectra of aliquots quenched at 15, 30, or 60 min with EDTA; errors $\pm$ 2%. [d] k_{D+} = 1.3 × 10^{-7} s^{-1} for the acid-catalyzed cleavage of **7** at pD 1.7−2.2; see text. [e] See text.

observed over 5 half-lives with k_{obs} = 4.0 × 10^{-4} s^{-1} (Hf^{4+}) and 4.4 × 10^{-4} s^{-1} (Zr^{4+}). These values appear in Table 1.

Contrasting behavior is found for Ce^{4+} and Th^{4+}. Th^{4+} cleaves DMPF only at C−OMe, affording *P*-monester **15**, which is stable to Th^{4+} for at least 5 days. In the ^{1}H NMR, MeOD (δ 3.33) and the doublet of **15** at δ 3.74 grow in as DMPF decays; P−OMe scission to **14** is not competitive. In the ^{31}P NMR, formation of **15** is signaled by growth of a broad signal at δ 6.3;[19] spiking with authentic **15** supported this assignment. Similarly, Th(IV) produces only product **15** when the cleavage of DMPF is carried out in H$_2$O instead of D$_2$O.

With Ce^{4+} a similar pattern ensues: DMPF decays in favor of **15** (^{1}H NMR doublet at δ 3.61[19]) and MeOH. However, precipitation occurs after ~1000 s, so that the rate constant, k_{obs} = 5.2 × 10^{-4} s^{-1}, is obtained from the initial rate. About 10% of *C*-monoester **14** also forms by Ce^{4+} P−OMe cleavage of DMPF.

We also observed M^{4+}-mediated reactions of the monoesters **14** and **15**. Zr^{4+} and Hf^{4+} slowly cleaved *C*-monoester **14** to PFA (**1**) [^{31}P at δ 4.2], with rate constants 2.2 × 10^{-6} s^{-1} and 2.6 × 10^{-6} s^{-1}, respectively. Zr^{4+} and Hf^{4+} induced decarboxylation of *P*-monoester **15** to *D*-phosphonate **16**.[21] Further

(21) ^{31}P NMR: δ 9.03 (t, J_{P-D} = 98 Hz). This signal becomes a triplet of quartets in the ^{1}H-coupled spectrum.

hydrolysis of **16** then led to MeOH release and the formation of DPO$_3$D$^-$.[22] The rate constants for this latter reaction, measured by MeOH release, were 2.4×10^{-5} s^{-1} (Zr) and 2.1×10^{-5} s^{-1} (Hf). About 10% of PFA also formed in these reactions.

Th^{4+} slowly cleaves *C*-monoester **14** with $k_{obs} = 4.2 \times 10^{-5}$ s^{-1}. PFA appears to be the final product of this reaction as identified by ^{31}P NMR with tartrate added to chelate Th(IV). Ce^{4+} induces net hydrolysis and decarboxylation of **14** to phosphate anion (^{31}P δ 2.1) with $k_{obs} = 9.3 \times 10^{-5}$ s^{-1}. PFA is stable to Ce^{4+}. With *P*-monoester **15**, Ce^{4+} induces decarboxylation to methyl phosphate (**17**) (^{31}P δ 3.07, q, $J_{P-H} = 10.8$ Hz).

In Scheme 2, we collect the set of reactions described above. Here, branch A pertains to initial P–OMe scission, whereas branch B comprises reactions that involve initial C–OMe cleavage. Rate constants for reactions of DMPF and *C*-monoester **14**, as well as **14**/**15** distributions, appear in Table 1.

Control experiments with DCl/D$_2$O furnished rate constants for the acid-catalyzed hydrolysis of DMPF in the *absence* of M^{4+}. At pD 1.7, 1.9, and 2.2, $k_{obs} = 1.35$, 1.42, and 1.21×10^{-7} s^{-1}, respectively (average $k_{obs} = 1.32 \times 10^{-7}$ s^{-1}). The products at pD 1.7 were *D*-phosphonate **16** from C–OMe cleavage followed by decarboxylation; subsequent hydrolysis produced DPO$_3$D anion.

With $k_{D+} = 1.3 \times 10^{-7}$ s^{-1} for the acid-catalyzed hydrolysis of DMPF, we find that the M^{4+}-mediated hydrolyses occur ~1000–4000 times more rapidly, as shown in Table 1.[23] Note, however, that acid catalysis induces only C–OMe scission and is more akin to the Th^{4+}- and Ce^{4+}-mediated cleavages than the Zr^{4+} and Hf^{4+} reactions in which P–OMe scission is the major pathway (Scheme 2).

In summary, Zr(IV) and Hf(IV) are chemoselective for the P–OMe cleavage of DMPF, whereas Th^{4+} and Ce^{4+} direct C–OMe scission. This pattern recurs in cleavages of monoesters **14** and **15**: *P*-monoester **15** is not appreciably cleaved by Th-(IV) or Ce(IV), but *C*-monoester **14** is cleaved 16–42 times more rapidly by Th(IV) or Ce(IV) than by Zr(IV) or Hf(IV).

Methoxycarbonyl Phenyl Phosphonate (8). Given the P–OMe chemoselectivity toward DMPF expressed by Zr(IV) and Hf(IV), it is reasonable to expect analogous selectivity in the phosphorolysis of substrate **8**, where the *P*-ester bears the more reactive phenoxide leaving group. This expectation is fulfilled.

Zr(IV)- and Hf(IV)-mediated hydrolyses of **8** in D$_2$O at pD 1.7 or 2.2 occur with $k_{Zr} = 2.33 \times 10^{-2}$ s^{-1} and $k_{Hf} = 0.65 \times 10^{-2}$ s^{-1}, respectively; see Table 2.[24] We note greater reactivity of **8** compared to the P–OMe scission of DMPF. Thus, the Zr(IV) and Hf(IV) P–OPh cleavages of **8** were too fast to be followed by NMR and required UV monitoring. The UV rate constants are not directly comparable to those obtained by ^{1}H NMR because the ratio of metal cation/substrate is much higher

(22) ^{31}P NMR: δ 3.2 (t, $J_{P-D} = 97$ Hz).
(23) DMPF is ~10^5–10^7 times more reactive than phosphodiesters (e.g., **5**), probably because of ground-state destabilization due to unfavorable carbonyl/phophoryl electronic interactions.[5b,d] Therefore, the catalytic enhancement of DMPF hydrolysis at P–OMe by M^{4+} is compressed (~10^3) relative to the much larger enhancements observed with **5**.[10]
(24) Kinetics were monitored by UV spectroscopy, following the release of phenol at 260, 270, or 280 nm. Reactions were pseudo-first-order over 5 half-lives.

Table 2. Kinetic Data for Phosphonoformates **8** and **18**[a]

M(IV)	$10^2 k_{obs}$ (s^{-1})		product distributions for cleavage of **8** (%)[b]	
	8	**18**	**14**	**18**
Zr[c]	2.33	1.54	>95	
Hf[c]	0.65	1.05	>95	
Th	0.016[d]	0.0026[c]		>95

[a] Conditions: as those in Table 1 (*a*), except [substrate] = 0.2 mM for UV kinetics (10 mM for NMR kinetics). [b] Product distributions determined by ^{31}P NMR of solutions after quenching with EDTA or tartrate. [c] Kinetics by UV monitoring of PhOH release at 260, 270, and 280 nm. [d] Kinetics by ^{1}H NMR in D$_2$O solution following disappearance of substrate C–OMe.

in the UV experiment. Qualitatively, however, P–OPh cleavage of **8** is faster than P–OMe cleavage of DMPF. ^{1}H NMR confirms the production of phenol in the cleavages of **8**; only traces of MeOD appear after full release of the phenol. Product **14** is exclusively formed (^{31}P δ −5.2); no **18** (^{31}P δ −1.18), the product of C–OMe cleavage, forms in these reactions (see Scheme 3).
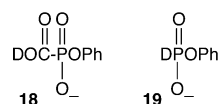
Although **18** does not form from **8** by Zr(IV)- or Hf(IV)-mediated cleavages, these cations do rapidly cleave **18**: k_{obs}-(Zr) $= 1.5 \times 10^{-2}$ s^{-1} and k_{obs}(Hf) $= 1.05 \times 10^{-2}$ s^{-1}, as determined by released phenol (UV). *D*-phosphonate **19** and DPO$_3$D$^-$ are the products, according to ^{31}P NMR, along with a trace of PFA (analogously to the Zr(IV) or Hf(IV) cleavage of *P*-monoester **15**; cf. Scheme 2).

The intriguing question with substrate **8** is whether Th(IV), which manifests C–OMe specificity toward DMPF, will maintain that selectivity despite the availability of a labile P–OPh linkage in **8**. In the event, C–OMe cleavage prevails.[25] Followed by ^{1}H NMR, Th^{4+} mediates hydrolysis of **8** (δ 3.83), yielding MeOD with $k_{obs} = 1.6 \times 10^{-4}$ s^{-1}, similar to $k = 1.3 \times 10^{-4}$ s^{-1} for the Th^{4+}-catalyzed C–OMe scission of DMPF (Tables 2 and 1). After 5 h, quenching of the reaction solution with tartrate (to remove Th^{4+}) reveals P-monoester **18** (and PFA) as the only products (^{31}P NMR).

P–OPh cleavage of **18** by Th(IV) is slower than C–OMe cleavage but does occur. UV-monitored phenol release gives $k_{obs} = 2.6 \times 10^{-5}$ s^{-1}. PFA is the product from P–OPh cleavage of **18**.

Table 2 collects rate constants pertaining to substrate **8**, while Scheme 3 summarizes the reactions. Note that the kinetic data for the M^{4+} cleavages of *C*-monoester **14** appear in Table 1 and are discussed in the section on DMPF hydrolysis.

The acid-catalyzed hydrolysis of **8** was followed by ^{1}H NMR spectroscopy, monitoring the decrease of substrate at pD 1.7 (DCl) in the absence of M^{4+}. We obtained $k = 1.1 \times 10^{-7}$ s^{-1}, similar to the D$^+$-catalyzed hydrolysis of DMPF (1.3×10^{-7} s^{-1}, see above), with DPO$_3$D$^-$ as the product. Rate enhancements of 10^3 (Th^{4+}) to 10^5 (Zr^{4+}) are obtained for the M(IV) cleavages of **8**, relative to D$^+$. Again, we note that the acid-catalyzed process (C–OMe cleavage, decarboxylation) differs from the P–OPh cleavage induced by Zr(IV) or Hf(IV). Most
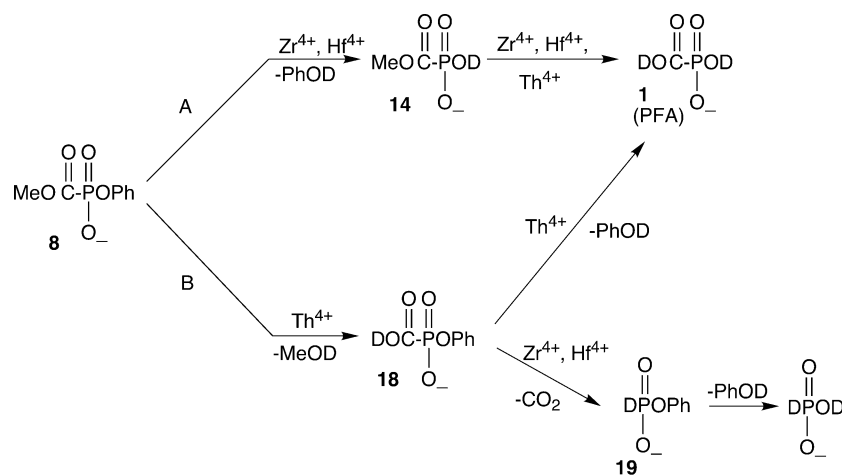
(25) Due to its proclivities for precipitation and substrate oxidation, Ce(IV) was not studied with this substrate.

Scheme 3

Table 3. Kinetic Data for Phosphonoformates **9** and **20**[a]

	$10^2 k_{obs}$ (s^{-1})		product distributions for cleavage of **9** (%)[b]	
M(IV)	**9**	**20**	**15**	**20**
Zr[c]	1.79	0.020	90	10
Hf[c]	0.61	0.011	79	21
Th[c]	0.18	0.24	>95	

[a] Conditions: as those in Table 1 (*a*), except [substrate] = 0.2 mM for UV kinetics (10 mM for NMR kinetics). [b] Product distributions determined by ^{31}P NMR of solutions after quenching with EDTA. [c] Kinetics by UV monitoring of phenol release at 260, 270, and 280 nm.

importantly, the chemoselectivity found with DMPF (P−OR cleavage by Zr(IV) or Hf(IV) but C−OR cleavage by Th(IV)) is maintained with substrate **8** and echoed by *P*-monoester **18** (Table 2), where P−OPh cleavage by Zr(IV) or Hf(IV) is 400−600 times faster than Th(IV) cleavage.

Phenoxycarbonyl Methyl Phosphonate (9). An important question to be answered here is whether the P−OR chemoselectivity of Zr(IV) and Hf(IV) is sufficiently robust to endure with substrate **9**, where the C−OPh site is highly labile. Followed by UV spectroscopic monitoring of released phenol in D$_2$O (conditions as above), Zr(IV)-, Hf(IV)-, and Th(IV)-mediated hydrolyses of **9** exhibited good pseudo-first-order behavior with $k_{Zr} = 1.79 \times 10^{-2}$ s^{-1}, $k_{Hf} = 0.61 \times 10^{-2}$ s^{-1}, and $k_{Th} = 0.18 \times 10^{-2}$ s^{-1}; see Table 3.

^{1}H NMR spectroscopy revealed that both MeOD (from P−OMe scission) and PhOD (from C−OPh scission) were liberated by Zr(IV) or Hf(IV). Correspondingly, *C*-monoester **20** and *P*-monoester **15** were produced in these reactions, as well as *D*-phosphonate **16**. These products were observed by
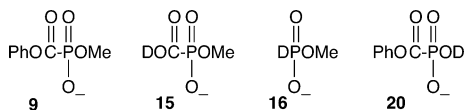
^{31}P NMR spectra obtained after 10 min of reaction (EDTA quench): δ 6.9 (**15**), −5.75 (**20**), and 9.0 (**16**).[21] After 50 min of reaction, only DPO$_3$D anion (from **16**) and PFA (from **20**) were present; see Scheme 4.

The distribution of **20**/**15** [P−OMe/C−OPh cleavage] was 10:90 for Zr^{4+} and 21:79 for Hf^{4+}, as determined from the ^{31}P NMR spectra at short reaction times. Thus, the P−OR chemoselectivity of Zr(IV) observed with (C−OMe) substrates **7** and **8**

does not persist with (C−OPh) substrate **9**. Nevertheless, it is remarkable that the P−OMe ester of **9** is at all cleaved by Zr-(IV) or Hf(IV) in competition with the C−OPh ester, considering the differences in leaving group and carbonyl vs phosphoryl site reactivities. Both differences favor *C*-esterolysis, so that the *P*-selective character of Zr(IV)- and Hf(IV)-mediated cleavages *persists*, even if *P*-esterolysis does not *dominate* with substrate **9**.

Reactions of *C*-monoester **20** with Zr(IV) or Hf(IV) proceed with $k_{Zr} = 2.0 \times 10^{-4}$ s^{-1} and $k_{Hf} = 1.1 \times 10^{-4}$ s^{-1}, with the release of phenol followed by UV spectroscopy. Only PFA is produced after 8 h of reaction at 25 °C with either metal cation. As expected, these C−OPh scissions of **20** to PFA are faster than the corresponding conversions of C−OMe monoester **14** ($k_{Zr} = 2.2 \times 10^{-6}$ s^{-1}, $k_{Hf} = 2.6 \times 10^{-6}$ s^{-1}; see Table 1). Cleavage of **20** with Th^{4+} affords only PFA with $k_{Th} = 0.24 \times 10^{-2}$ s^{-1}.

Reaction of diester **9** with Th^{4+} (0.18×10^{-2} s^{-1}) gives only C−OPh scission to phenol and *C*-monoester **15** (^{1}H and ^{31}P NMR described above). Given the *C*-esterolytic chemoselectivity of Th^{4+} and the good C−OPh leaving group of **9**, this result is unsurprising. Scheme 4 outlines the reactions described in this section. The reactions of Zr(IV) and Hf(IV) with **15** are discussed above in connection with DMPF.

Acidic hydrolysis of **9** (to **16** and DPO$_3$D$^-$) at pD 1.7 (HCl) occurs with $k_{D^+} = 6.2 \times 10^{-7}$ s^{-1}, as followed by NMR spectroscopy of the substrate. Therefore, M^{4+} catalysis of the cleavage of **9** occurs with enhancements of ~2.9×10^4 (Zr^{4+}) to 2.9×10^3 (Th^{4+}).
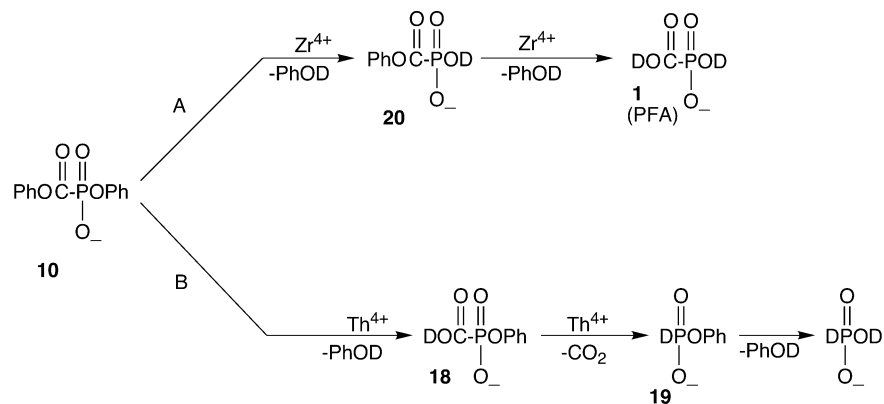
Diphenyl Phosponoformate (10). Finally, we examined the Zr^{4+}- and Th^{4+}-mediated hydrolyses of diphenyl phosphonoformate (**10**). Unfortunately, 10 mM **10** immediately precipitated with 25 mM Zr(IV) or Th(IV), our standard concentrations. It was necessary to use a 1:1 D$_2$O/CD$_3$CN mixture as the solvent for reactions of **10**.

The cleavage of **10** ([31]P δ −8.85) by Zr^{4+}, followed by ^{1}H NMR and ^{31}P NMR, revealed the formation of phenol (δ 7.25−7.34) and *C*-monoester **20** ([31]P δ −5.25[19]), the products of P−OPh scission; see Scheme 5, branch A. No other signals were observed, so that the Zr(IV)-mediated hydrolysis of **10** was chemospecific at P−OPh. UV monitoring of released phenol gave $k_{Zr} = 1.29 \times 10^{-2}$ s^{-1} for the P−OPh cleavage of **10** by Zr^{4+} with [**10**] = 0.2 mM and [Zr^{4+}] = 25 mM; see Table 4.

Scheme 4

Zr⁴⁺, Hf⁴⁺ / −MeOD → PhOC-POD (**20**)
Zr⁴⁺, Hf⁴⁺ / −PhOD → DOC-POD (**1**, PFA)

A

PhOC-POMe (**9**)

B

Th⁴⁺, Zr⁴⁺, Hf⁴⁺ / −PhOD → DOC-POMe (**15**)
Zr⁴⁺, Hf⁴⁺ / −CO₂ → DPOMe (**16**)
−MeOD → DPOD

Scheme 5

Zr⁴⁺ / −PhOD → PhOC-POD (**20**)
Zr⁴⁺ / −PhOD → DOC-POD (**1**, PFA)

A

PhOC-POPh (**10**)

B

Th⁴⁺ / −PhOD → DOC-POPh (**18**)
Th⁴⁺ / −CO₂ → DPOPh (**19**)
−PhOD → DPOD
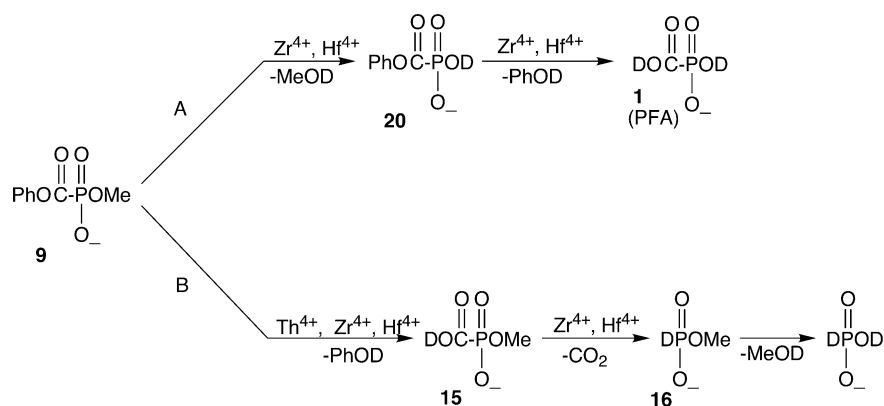
Table 4. Kinetic Data for Phosphonoformate **10**[a]

M(IV)	$10^2 k_{obs}$ (s⁻¹)	product distributions for cleavage of 10 (%)[b]	
		18	**20**
Zr[c−e]	1.29		>95
Th[c−e]	0.47	90	10

[a] Conditions: as those in Table 1 (*a*), except [substrate] = 0.2 mM for UV kinetics (10 mM for NMR studies). [b] Product distributions determined by ³¹P NMR of solutions after quenching with EDTA. [c] Kinetics by UV monitoring of phenol release at 270 nm. [d] For kinetic data of **18** and **20**, see text and Tables 2 and 3. [e] Solvent is 1:1 MeCN/D₂O for product studies but D₂O for UV kinetic studies.

This rate constant is similar to that for the analogous P−OPh cleavage of **8** (see Table 2). Continued incubation with Zr⁴⁺ led to slow cleavage of **20** to PFA, as verified by ³¹P NMR, with $k = 7.54 \times 10^{-4}$ s⁻¹ (UV). This value is somewhat higher than the one observed in the direct reaction of **20** with Zr⁴⁺ (2.0×10^{-4} s⁻¹, Table 3).

In contrast, reaction of **10** with Th⁴⁺ gave mainly *P*-monoester **18** via C−OPh scission, verified by ³¹P NMR spiking experiments; see Scheme 5, branch B. About 10% of **20** was also observed in this cleavage. UV monitoring of released phenol gave $k_{Th} = 4.72 \times 10^{-3}$ s⁻¹. Continued incubation with Th⁴⁺ converted **18** to *D*-phosphonate **19** (³¹P δ 3.3, t, $J_{P-D} = 99$ Hz) by decarboxylation and then to DPO₃D anion by the hydrolytic loss of phenol. The UV-determined rate constant for the latter reaction was 1.05×10^{-4} s⁻¹. It is of interest that the Th(IV) cleavage of **18** in D₂O gives PFA (Scheme 3), whereas decarboxylation to **19** prevails in CD₃CN/D₂O.

The main result, as portrayed in Table 4 and Scheme 5, is that the Zr(IV) or Th(IV) hydrolyses of **10** manifest opposite P−OPh vs C−OPh chemoselectivities, respectively, in parallel to their behavior with substrate **7** (DMPF); see Table 1.

A control experiment in which DMPF was cleaved by Zr⁴⁺ in 1:1 CD₃CN/D₂O gave P−O scission to **14** and C−O scission to **15** (see Scheme 2) in a ratio of 37:63 as determined by ³¹P NMR. The P−OMe/C−OMe chemoselectivity of 80:20 observed for Zr⁴⁺ in 100% D₂O (Table 1) is thus "reversed" in CD₃CN/D₂O. Substrate cleavage is also ∼4.5 times slower (0.96×10^{-4} s⁻¹, ¹H NMR) in the binary solvent, compared to D₂O (4.4×10^{-4} s⁻¹). This influence of solvent on the chemoselectivity of the Zr(IV)-mediated hydrolysis may reflect solvent effects on the stabilities of the Zr⁴⁺ complexes that are responsible for the P−O selectivity (see Discussion).

Th⁴⁺ cleavage of DMPF in 1:1 CD₃CN/D₂O gave only C−OMe scission to **15**, as in D₂O alone, and with an almost unchanged rate constant (1.16×10^{-4} s⁻¹ by ¹H NMR vs 1.3×10^{-4} s⁻¹ in D₂O, Table 1). Th⁴⁺-mediated hydrolysis is thus unaffected by the solvent change.

We also carried out rate constant vs M(IV) concentration studies, from which a correlation of log k vs log[M(IV)] might reveal the reaction order in metal cation. We performed these experiments for substrate **8** with Zr(IV) and substrate **9** with Th(IV), but we could not conveniently do so for DMPF (**7**), where the dual necessities of a minimum substrate concentration for NMR analysis and a high [M(IV)]/substrate ratio to ensure pseudo-first-order behavior would require impractically high metal ion concentrations.

With **8**−Zr(IV) and **9**−Th(IV), full P−OPh and C−OPh cleavage selectivity (respectively) was observed (see above). The kinetics of cleavage were readily followed by UV monitoring of the released phenol in both D₂O and H₂O, which

permitted the evaluation of an *apparent* solvent isotope effect. In these experiments, the maximum [M(IV)] = 25 mM, [**8** or **9**] = 0.2 mM, [NaClO$_4$] = 0.5 M, and the solution pH or pD was established by the natural hydrolysis of M(IV) at 25 mM, with the pH or pD adjusted at lower metal ion concentrations by the addition of DCl or HCl as required.

The dependence of k_{obs} on the cleavage of **8** by Zr(IV) in H$_2$O at pH 1.0 showed linear behavior within the range of metal ion concentrations employed ($\sim$2.5−25 mM). The same reaction in D$_2$O at pD 1.7 displayed linear behavior at lower concentrations of metal ion, with some saturation beginning at higher concentrations (see Figure S1 in the Supporting Information). The second-order rate constants were k_2 = 0.86 ± 0.03 M^{-1} s^{-1} in H$_2$O and 1.29 ± 0.06 M^{-1} s^{-1} in D$_2$O. From these results the apparent solvent isotope effect, k_2(H$_2$O)/k_2(D$_2$O) = 0.66. Although the difference between pH (1.0) and pD (1.7) complicates a mechanistic interpretation, it seems clear that the H$_2$O to D$_2$O change does not cause a major alteration in the mechanism. Figure S2 shows the dependence of log k_{obs} vs log-[Zr(IV)] for the cleavage of **8** in both H$_2$O and D$_2$O at 25 °C and 0.5 M NaClO$_4$; good linear behavior was observed with slopes of 0.84 ± 0.01 and 0.79 ± 0.03, respectively.

In contrast to the **8**−Zr results, the dependence of k_{obs} for the cleavage of **9** by Th(IV) in H$_2$O at pH 2.3 showed saturation with increasing [Th(IV)]. Saturation was also observed in D$_2$O at pD 2.9. (See Figure S3 in the Supporting Information.) Apparent second-order rate constants could be estimated from the linear portions of the curves, affording k_2 = 0.44 ± 0.03 M^{-1} s^{-1} in H$_2$O and 0.66 ± 0.01 M^{-1} s^{-1} in D$_2$O. For this system too, an apparent solvent isotope effect of 0.66 is obtained. The apparent reaction order can be extracted from the linear portions of the curves. Figure S4 (Supporting Information) shows the dependence of log k_{obs} on log[Th(IV)] for the cleavages of **9** in H$_2$O (pH 2.3) and D$_2$O (pD 2.9) at 25 °C and 0.5 M NaClO$_4$. The slopes calculated from the linear fit were 0.82 ± 0.04 and 0.84 ± 0.06, respectively. We will return to the log k_{obs} vs log[M(IV)] results in the Discussion section.

Finally, we note that the saturation kinetics observed for the **9**/Th(IV) system, in comparison to the linear behavior exhibited by **8**/Zr(IV), reflects differences in the degree of protonation of the substrates under the experimental conditions where their kinetics are measured. PFA diesters such as **8** and **9** should have pK_a's similar to the first pK_a of the parent PFA ($\sim$0.78). Therefore, at pH 1.0, substrate **8** should be $\sim$30% in the protonated form, decreasing its apparent binding to the metal cation. In contrast, at pH 2.3, substrate **9** should be fully deprotonated and display saturation at a lower concentration of metal ion.

Discussion

Dominant Forms of the Hydroxo-Metal Species. Ce(IV), Th(IV), Zr(IV), and Hf(IV) catalyze cleavages of phosphono-formate substrates **7**−**10** by $\sim$3−4 orders of magnitude. Moreover, the cations manifest an unprecedented chemoselec-tivity in which Ce(IV) and Th(IV) favor C−OR scission, whereas Zr(IV) and Hf(IV) prefer P−OR cleavage (given identical leaving groups at both C−OR and P−OR, e.g., R = Me or Ph). In this discussion we will consider these issues of chemoselectivity and catalysis.

The well-known ability of metal ions to activate coordinated water molecules (i.e., to decrease the pK_a of water) leads to the formation of polynuclear hydroxo-metal species.[26,27] At sufficiently low concentration ($<1 \times 10^{-5}$ M), cations generally appear to give mononuclear hydroxo species, but, at ordinary concentrations ($>1 \times 10^{-3}$ M), they often produce several polymeric species. Polynuclear hydroxo-complex formation is established or suspected for the great majority of 3+ and 4+ ions, as well as for many 2+ ions.[27] Thus, at concentrations from 1 mM to 25 mM in weakly acidic solutions, metal ions such as Ce(IV) and Zr(IV) are most likely present as discrete polynuclear hydroxo species rather than as simple aquocations [M(H$_2$O)$_x$]$^{4+}$ or the related monohydroxo species [M(OH)-(H$_2$O)$_{x-1}$]$^{(4-1)+}$.

Despite much effort, identification of these polymeric species has been difficult, in part due to the necessity of operating within narrow concentration and pH ranges. There are only a few detailed studies of phosphate and phosphonate ester cleavage that characterize the active species of tri- or tetravalent metal cations in solution.[28−30] To rationalize their chemoselectivity, we need to understand the aqueous solution chemistry and polynuclear hydroxo-metal species of Ce(IV), Th(IV), Zr(IV), and Hf(IV). We make use of the available literature data,[26,27,31] noting that a particularly detailed account of metal ion polym-erization is offered by Baes and Mesmer.[27]

A. Ce(IV). Based on several studies of Ce(IV) salts, with both perchlorate and nitrate counterions, Baes and Mesmer describe the formation of several Ce(IV) species as represented by the set of equilibria in Chart 1.[27] The log $K_{n,m}$ data of Chart 1 can be processed by the program SPE given by Martell and Motekaitis[32] to afford the distribution of equilibrium concentra-tions of the various Ce(IV) species at selected values of [Ce-(IV)]$_{total}$ and pH. The SPE program approximates the degree of formation of each metal ion species depending on a given set of stability constants, total metal ion concentration, and solution pH. Program output includes a "complete listing of each species, its stoichiometry, concentration, and relative percentages all as a function of pH."[32] A detailed discussion, complete program code, and appropriate floppy disks are contained in ref 32. We thus obtain [Ce(IV)] species distributions as a function of pH which can be converted to the format of Figure 1 using the program *Origin 4.0* (Microcal).

At pH $\sim$2, dimeric and hexameric Ce(IV) species are predicted to dominate. Structural information is scarce, although hexanuclear Ce$_6$(OH)$_{12}$$^{12+}$ has been related to the crystal structure of Ce$_6$O$_4$(OH)$_4$(SO$_4$)$_6$, in which 6 Ce^{4+} ions are in an octahedral arrangement, and each of the four O^{2-} and OH$^-$ ions are centered on the octahedral faces.[27] Interestingly, in recent studies on the cleavage of cyclic adenosine 3′,5′-monophosphate (cAMP) by Ce(IV) acidic solutions, Komiyama and co-workers

(26) (a) Burgess, J. *Metal Ions in Solution*; Halstead Press: New York, 1978. (b) Burgess, J. *Ions in Solution: Basic Principles of Chemical Interactions*; Ellis Horwood: New York, 1988. (c) Choppin, G. R. *Radiochim. Acta* **1983**, *32*, 43.
(27) Baes, C. F., Jr.; Mesmer, R. E. *The Hydrolysis of Cations*; Wiley-Interscience: New York, 1976.
(28) Komiyama, M.; Takeda, N.; Shigekawa, H. *Chem. Commun.* **1999**, 1443.
(29) Blewett, F. McC.; Watts, P. *J. Chem. Soc. B* **1971**, 881.
(30) Hurst, P.; Takasaki, B. K.; Chin, J. *J. Am. Chem. Soc.* **1996**, *118*, 9982.
(31) Smith, R. M.; Martell, A. E. *Critical Stability Constants*, Plenum Press: New York, 1976; Vol. 4−6.
(32) Martell, A. E.; Motekaitis, R. J. *Determination and Use of Stability Constants*, 2nd ed.; VCH: New York, 1992; p 173. The "SPE" program was supplied as a floppy disk that accompanied the book and was implemented on our PC.

Chart 1. Equilibria for Ce(IV)[a]

				Equilibria			$K_{n,m}$	$\text{Log}K_{n,m}$[b]
Ce^{4+}	+	H_2O	$\rightleftharpoons$	$Ce(OH)^{3+}$	+	H^+	$K_{1,1}$	1.1 (−1.8)
Ce^{4+}	+	$2H_2O$	$\rightleftharpoons$	$Ce(OH)_2^{2+}$	+	$2H^+$	$K_{1,2}$	0.3 (−2.6)
$2Ce^{4+}$	+	$2H_2O$	$\rightleftharpoons$	$Ce_2(OH)_2^{6+}$	+	$2H^+$	$K_{2,2}$	3.6 (−2.2)
$2Ce^{4+}$	+	$3H_2O$	$\rightleftharpoons$	$Ce_2(OH)_3^{5+}$	+	$3H^+$	$K_{2,3}$	4.1 (−1.7)
$2Ce^{4+}$	+	$4H_2O$	$\rightleftharpoons$	$Ce_2(OH)_4^{4+}$	+	$4H^+$	$K_{2,4}$	3.5 (−3.39)
$6Ce^{4+}$	+	$12H_2O$	$\rightleftharpoons$	$Ce_6(OH)_{12}^{12+}$	+	$12H^+$	$K_{6,12}$	15.4 (−1.98)
Ce^{4+}	+	$2H_2O$	$\rightleftharpoons$	$CeO_2(s)$	+	$4H^+$	$K_{1,0}$	−8.2

[a] Data and equations are taken from ref 27, Tables 7.3 and 7.4, and the discussion on pp 139−146. [b]Values at $I = 3$ M (ClO_4^-). In parentheses, values at $I = 3$ M (NO_3^-). Data unavailable for recalculation at $I = 0.5$.[27]
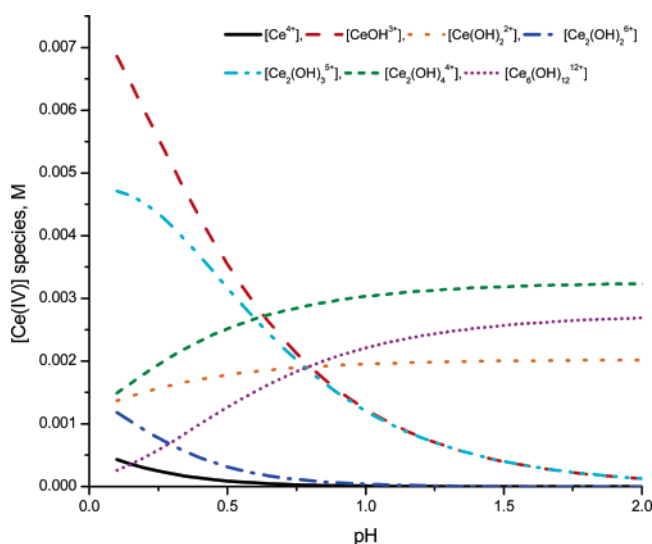

Figure 1. Speciation of Ce(IV) as a function of pH, with [Ce(IV)] = 0.025 M, $I = 3$ M (ClO_4^-). The equilibrium concentrations of each Ce(IV) species at each pH were calculated from the equilibrium constants in Chart 1 (taken from ref 27), using the iterative program SPE (see ref 32). A description of this program appears in the text.

directly correlate the observed reactivity with the dimeric Ce-(IV)-hydroxo species $[Ce^{IV}_2(OH)_4]^{4+}$.[28,33]

B. Th(IV). From very careful potentiometric studies with ClO_4^-, Cl^-, and NO_3^- counterions, as well as studies with other techniques including ultracentrifugation, light scattering, and X-ray scattering, Baes and Mesmer represent the formation of various Th(IV) species by the equilibria in Chart 2.[27] As with Ce(IV), speciation diagrams can be calculated[32] from these equilibrium constants for different concentrations of Th(IV). Figure 2 depicts the results with [Th(IV)] = 0.025 M. At pH 3, both monomeric and dimeric Th(IV) species exist. The dimer $Th_2(OH)_2^{6+}$ appears in studies with all 3 counterions[27] and is strongly supported by X-ray scattering results in which two bridging hydroxides link the metal centers with a Th−Th distance of 3.95 Å.[26a]

C. Zr(IV) and Hf(IV). The chemistry of zirconium (IV) salts has been studied extensively in acidic aqueous solutions using various instrumental techniques, including protometry,[34] small-

angle X-ray scattering (SAXS),[35] ^{17}O and ^{1}H NMR,[36] Raman spectroscopy,[37] light scattering,[38] and ultracentrifugation.[39] Despite intense investigation, there is still debate about the exact nature of the species. Hafnium(IV) is much less studied; its chemistry is usually considered to be very similar to that of Zr(IV). Baes and Mesmer reviewed pre-1975 data[38−40] and proposed the set of equilibria shown in Chart 3 for Zr(IV) species.

This set of equilibria only indicates the overall metal-to-hydroxide stoichiometry of the species; no structural information is available in most of the cases except for $Zr_4(OH)_8^{8+}$, which is believed to exist as hydroxyl-bridged tetramers, $[Zr_4(OH)_8-(H_2O)_{16}(Cl_x)]^{(8-x)+}$ (**21**), similar to the unit in the crystal structure of $ZrOCl_2 \cdot 8H_2O$.

Based on the foregoing, it has been generally accepted that the predominant Zr(IV) species in acidic homogeneous aqueous solutions is the hydroxyl-bridged tetramer (**21**).[36,37] However, in a recent SAXS study, Singhal et al.[35c] showed that the tetramer was not the only species present. At 0.05 M $ZrOCl_2$ in aqueous solutions in the pH range 0.1−1.5, an equilibrium between tetramers $[Zr_4(OH)_8(H_2O)_{16}Cl_6]^{2+}$ and octamers $[Zr_8-(OH)_{20}(H_2O)_{24}Cl_{12}]$ was found (Chart 4, a) with a quotient, $Q = 0.2 \pm 0.05$ M (Chart 4, b). The octamer was proposed to exist in a stacked form comprised of two tetramers (cf., **22**, water molecules are omitted for clarity).[35c] Therefore, an additional equilibrium can be added to Chart 3, with a formation constant ($K_{8,20}$) calculated from $K_{4,8}$ and the quotient Q; cf., Chart 4, c and d.

Evaluation of the Zr(IV) species at equilibrium can now be made[32] using the stability constants ($K_{n,m}$) given in Charts 3 and 4 (d). The speciation for Zr(IV) at 0.025 M as a function of pH appears in Figure 3. Additionally, similar diagrams for different $[Zr(IV)]_o$ concentrations could be evaluated so that equilibrium concentrations for Zr tetramers and octamers as a function of the total [Zr] at a given pH could also be obtained; see Figure S5 in the Supporting Information.

(33) Sumaoka, J.; Takeda, N.; Okada, Y.; Takahashi, H.; Shigekawa, H.; Komiyama, M. *Nucleic Acid Symp. Ser.* **1998**, *39*, 137.

(34) Veyland, A.; Dupont, L.; Pierrand, J.-C.; Rimbault, J.; Aplincourt, M. *Eur. J. Inorg. Chem.* **1998**, 1765.
(35) (a) Hu, M. Z.-C.; Zielke, J. T.; Lin, J.-S.; Byers, C. H. *J. Mater. Res.* **1999**, *14*, 103. (b) Singhal, A.; Toth, L. M.; Beaucage, G.; Lin, J.-S.; Peterson, J. J. *Colloid Interface Sci.* **1997**, *194*, 470. (c) Singhal, A.; Toth, L. M.; Lin, J.-S.; Affholter, K. *J. Am. Chem. Soc.* **1996**, *118*, 11529.
(36) Åberg, M.; Glaser, J. *Inorg. Chim. Acta* **1993**, *206*, 53.
(37) Hannane, S.; Bertin, F.; Bouix, J. *Bull. Soc. Chim. Fr.* **1990**, *127*, 43.
(38) Angstadt, R. L.; Tyree, S. Y. *J. Inorg. Nucl. Chem.* **1962**, *24*, 913.
(39) Johnson, J. A.; Kraus, K. A. *J. Am. Chem. Soc.* **1956**, *78*, 3937.
(40) Zielen, A. J.; Connick, R. E. *J. Am. Chem. Soc.* **1956**, *78*, 5785.

Chart 2. Equilibria for Th(IV)[a]

			Equilibria			$K_{n,m}$	$\mathrm{Log}K_{n,m}$[b]
Th^{4+}	+	H_2O	$\rightleftharpoons$	$Th(OH)^{3+}$	+ H^+	$K_{1,1}$	-3.95
Th^{4+}	+	$2H_2O$	$\rightleftharpoons$	$Th(OH)_2^{2+}$	+ $2H^+$	$K_{1,2}$	7.25
Th^{4+}	+	$3H_2O$	$\rightleftharpoons$	$Th(OH)_3^{+}$	+ $3H^+$	$K_{1,3}$	-12.44
Th^{4+}	+	$4H_2O$	$\rightleftharpoons$	$Th(OH)_4$	+ $4H^+$	$K_{1,4}$	-16.64
$2Th^{4+}$	+	$2H_2O$	$\rightleftharpoons$	$Th_2(OH)_2^{6+}$	+ $2H^+$	$K_{2,2}$	-4.87
$4Th^{4+}$	+	$8H_2O$	$\rightleftharpoons$	$Th_4(OH)_8^{8+}$	+ $8H^+$	$K_{4,8}$	-19.41
$6Th^{4+}$	+	$15H_2O$	$\rightleftharpoons$	$Th_6(OH)_{15}^{9+}$	+ $15H^+$	$K_{6,15}$	-36.76
Th^{4+}	+	$2H_2O$	$\rightleftharpoons$	$ThO_2(s)$	+ $4H^+$	$K_{1,0}$	7.04

[a] Data and equations are taken from ref 27, Tables 8.5 and 8.8, and the discussion on pp 158–168. [b] Calculated at $I = 0.5$ M from equations in ref 27.
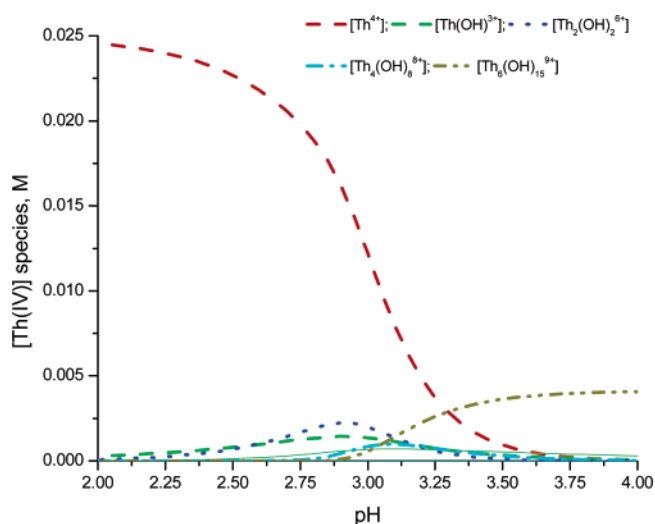
Figure 2. Speciation of Th(IV) as a function of pH, with [Th(IV)] = 0.025 M, $I = 0.5$ M (ClO_4^-). The equilibrium concentrations of each Th(IV) species at each pH were calculated from the equilibrium constants in Chart 2 (taken from ref 27), using the iterative program SPE (see ref 32). A description of this program appears in the text.
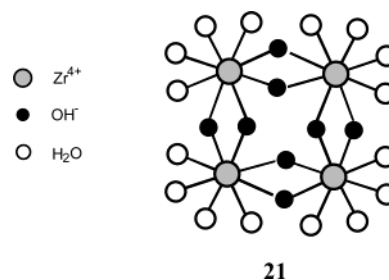
From Figure 3, we reach a conclusion similar to that of Singhal:[35c] the tetramer dominates at high acidity (pH 0–0.6), whereas the octamer is more prevalent in the 1.0–1.5 pH range. Under the latter conditions, other species are practically negligible. We should note that Zr speciation may be quite different at *low* Zr concentrations. For example, Aplincourt et al. found that with $8 \times 10^{-5} < [Zr] < 8 \times 10^{-3}$ M, species such as $Zr(OH)_3^+$, $Zr_2(OH)_7^+$, and $Zr(OH)_4$ may dominate.[34] Recent SAXS data strongly support polymeric species at $[ZrOCl_2] > 0.05$ M.[35] Unfortunately, there are no experimental data covering the concentration interval 8×10^{-3}–5×10^{-2} M.

Chemoselectivity. The preceding discussion indicates that, under the acidic conditions employed, dimeric or monomeric Ce(IV) and Th(IV) species and tetrameric or octameric Zr(IV) and (presumably) Hf(IV) species are the prevalent forms of the metal cations present during phosphonoformate diester hydrolysis. We have seen that Ce(IV) and Th(IV) foster *C*-ester scission, whereas Zr(IV) and Hf(IV) favor *P*-ester cleavage. Previously,[18] we associated this chemoselectivity with dimeric Ce(IV) and

Th(IV) species, as opposed to tetrameric or octameric Zr(IV) and Hf(IV) species. The hydrolytic models follow.

The chemoselectivity of cleavage for substrates **7**–**10** must depend on which M–OH species are present under the reaction conditions and the particular mode of substrate binding in each case. For the PFA diesters, which at pD 1.7–3.1 are present in aqueous solutions as the $P-O^-$ monoanions,[3] binding to the metal species (i.e., Lewis activation) and the simultaneous supply of a metal-bound hydroxide nucleophile to attack either the phosphoryl or the carbonyl groups must account for the observed hydrolytic accelerations in comparison with the acid-catalyzed reactions (see Tables 1–4).[30,42] However, it should be noted that D^+ induces only C–O ester scission and is more comparable to Th(IV) and Ce(IV), rather than to Zr(IV) and Hf(IV), which mainly display reactivity at the phosphoryl ester.

We represented[11,18,28] Ce(IV) cleavage of (e.g., DMPF) by **23**, where intramolecular hydroxide attack at the carbonyl center (*a*) occurs via a five-membered transition state, whereas attack at phosphorus (*b*) requires a more strained four-centered transition state.

21

This analysis suggests that C–O scission is kinetically preferred to P–O scission (given comparable leaving groups at C and P). By implication, other dimeric or monomeric metal complexes (cf., Th) should also be C–O selective. This is also the case for trivalent Co, La, and Eu; see below.

It is also possible to envisage cleavage of the bound phosphonoformate by a bridging hydroxyl group, cf. **24**.[17a,42,43]

(41) This includes acceleration of C–OMe scission. Ce(IV)-mediated cleavage of DMPF is 98 times faster than the analogous process for methyl acetate, where $k_{obs} = 5.3 \times 10^{-6}$ s^{-1}.
(42) Takasaki, B. K.; Chin, J. *J. Am. Chem. Soc.* **1995**, *117*, 8582.
(43) Moss, R. A.; McKernan, B. A.; Sauers, R. R. *Tetrahedron Lett.* **2002**, *43*, 5925.

Chart 3. Equilibria for Zr(IV)^a

				Equilibria				$K_{n,m}$	$\text{Log}K_{n,m}{}^b$
Zr^{4+}	+	H_2O	$\rightleftharpoons$	$Zr(OH)^{3+}$	+	H^+		$K_{1,1}$	-0.46
Zr^{4+}	+	$2H_2O$	$\rightleftharpoons$	$Zr(OH)_2{}^{2+}$	+	$2H^+$		$K_{1,2}$	-2.02
Zr^{4+}	+	$3H_2O$	$\rightleftharpoons$	$Zr(OH)_3{}^+$	+	$3H^+$		$K_{1,3}$	-5.84
Zr^{4+}	+	$4H_2O$	$\rightleftharpoons$	$Zr(OH)_4$	+	$4H^+$		$K_{1,4}$	-16.44
Zr^{4+}	+	$5H_2O$	$\rightleftharpoons$	$Zr(OH)_5{}^-$	+	$5H^+$		$K_{1,5}$	-16.57
$3Zr^{4+}$	+	$5H_2O$	$\rightleftharpoons$	$Zr_3(OH)_5{}^{7+}$	+	$5H^+$		$K_{3,5}$	4.97
$4Zr^{4+}$	+	$8H_2O$	$\rightleftharpoons$	$Zr_4(OH)_8{}^{8+}$	+	$8H^+$		$K_{4,8}$	7.69
Zr^{4+}	+	$2H_2O$	$\rightleftharpoons$	$ZrO_2(s)$	+	$4H^+$		$K_{1,0}$	-1.15

^{a} Data and equations are taken from ref 27, Tables 8.3 and 8.4, and the discussion on pp 155−158. ^{b}Calculated at $I = 0.5$ M from equations in ref 27.

Chart 4. Additional Equilibria for Zr(IV)

(a) $2[Zr_4(OH)_8(H_2O)_{16}Cl_6{}^{2+}] \rightleftharpoons [Zr_8(OH)_{20}(H_2O)_{24}(Cl_{12})] + 4H_2O + 4H^+$

(b) $Q = [Zr_8(OH)_{20}(H_2O)_{24}Cl_{12}][H^+]^4/[Zr_4(OH)_8(H_2O)_{16}Cl_6{}^{2+}]^2$

(c) $\text{Log } K_{8,20} = \text{Log } Q + 2 \text{ Log } K_{4,8}$

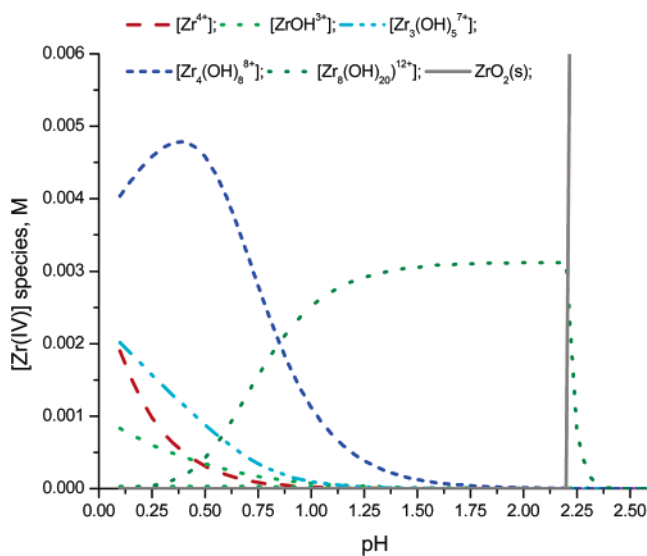(d) $8Zr^{4+} + 20 H_2O \rightleftharpoons Zr_8(OH)_{20}{}^{12+} + 20H^+$ $\text{Log } K_{8,20} = 14.7$

Figure 3. Speciation of Zr(IV) as a function of pH, with [Zr(IV)] = 0.025 M, $I = 0.5$ (ClO$_4$$^-$). The equilibrium concentrations of each Zr(IV) species at each pH were calculated from the equilibrium constants in Charts 3 and 4 (taken from ref 27), using the iterative program SPE (see ref 32). A description of this program appears in the text.

Again, *C*-attack corresponds to a (nominally) five-membered ring transition state (or intermediate), while *P*-attack transits a four-membered cycle. Examples of **24** and related constructs with M = La were examined computationally, and preferred *C*-ester attack was indicated.[43]

For Zr(IV) we expect octamers **22** to be the dominant species at pD 1.5−1.7;[27,32,35c] cf. Figure 3. The octamers are most readily represented as stacked hydroxyl-bridged tetramers,[35c] which also occur as the unit cell in the crystal structure of ZrOCl$_2$·8H$_2$O.[44] Binding of DMPF to the Zr(IV) octamer can be represented as that in **25**, where intracomplex OH$^-$ cleavage can now readily

occur at phosphorus via a six-membered transition state. The

22
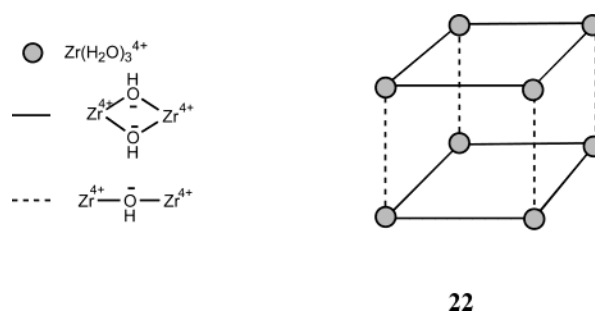
tripodal phosphonate product (**26**) reproduces the binding scheme of the lamellar zirconium phosphonates.[45] Cleavage of DMPF by Hf(IV), which also affords P−O selective cleavage, must follow an analogous mechanism.[20]

A. What Evidence Supports These Models? The mechanism represented by **25** → **26** implies that alteration of the Zr-(IV) octamers should impact the expressed P−O chemoselectivity. Tris(2-hydroxymethyl)aminomethane (**27**) is reported to form 1:1 complexes with Zr(IV) that are able to cleave bis-*p*-nitrophenyl phosphate in acidic aqueous solution.[46] Indeed, addition of 1 or 2 equiv of **27** to the Zr reaction mixture of Table 1 changes the **14**/**15** product distribution from ~80:20 to 40:60 or 15:85, respectively; the P−O chemoselectivity shifts to C−O selectivity. With Hf(IV), similar additions of 1 or 2 equiv of **27** change the **14**/**15** distribution from 90:10 (Table 1) to 66:34 or 19:81, respectively.[47]

Note that the interaction of **27** with Zr only occurs via the tris-alcohol functionality; the amino group must be deuterated under the reaction conditions. The addition of **27** raised the solution pD by 0.2−0.6, so that we also examined the effect of adding 1 equivalent of NaOD to the Zr(IV) or Hf(IV) solutions (2 equivalents of NaOD induced turbidity). Again, the **14**/**15** distributions changed, shifting to 50:50 (Zr) or 58:42 (Hf). The addition of small quantities of NaOH to aqueous Zr(IV) solutions is known to promote the formation of higher oligo-

(44) Mark, T. C. *Can. J. Chem.* **1968**, *46*, 3493.
(45) (a) Amicangelo, J. C.; Leestra, W. R. *J. Am. Chem. Soc.* **1998**, *120*, 6181. (b) Mitchell, M. C.; Kee, T. P. *Coord. Chem. Rev.* **1997**, *158*, 359 and especially 362, 363. (c) Clearfield, A. *Prog. Inorg. Chem.* **1998**, *47*, 371.
(46) Ott, R.; Krämer, R. *Angew. Chem., Int. Ed.* **1998**, *37*, 1957.
(47) Control experiments show that, in the absence of M(IV), added Tris does not cleave DMPF at pD 2.2 over 72 h at 25 °C.

23   **24**
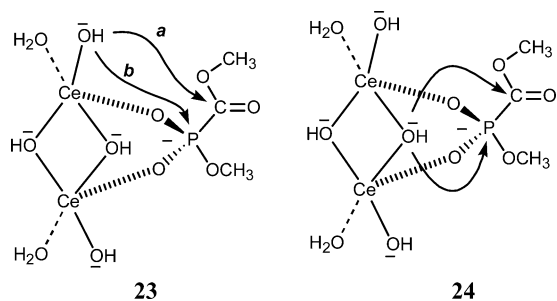
meric Zr species.[48] Thus, the P−O selectivity of Zr(IV) and Hf(IV) toward DMPF appears to be a property of M(IV) tetramers or octamers and can be shifted toward C−O selectivity by modifying these complexes. We can also imagine that the use of 1:1 acetonitrile/water as the solvent, necessary for substrate **10**, would perturb the speciation of Zr(IV) and alter the P−O/C−O regiochemistry of DMPF cleavage (see above).

These speciation and binding models help rationalize the opposing hydrolytic chemoselectivities expressed by Ce(IV) and Th(IV) or Zr(IV) and Hf(IV) toward substrates **7−10**. By implication, other dimeric or monomeric metal complexes (or simple nucelophilic reagents) should, like Ce(IV) or Th(IV), be C−O selective. We have found that Eu(III) and La(III) cations, and their bis-tris propane complexes, do indeed mediate the hydrolysis of DMPF with C−OMe chemospecificity and substantial rate enhancement.[43,49] These lanthanide metal complexes are most likely dimers.[27,30,42,43]

Similarly, 10 mM DMPF was hydrolyzed at pD 6.8 by 25 mM of the monomeric Co(III)cyclen complex **28** [15,50] with k_{obs} = 9.5 × 10⁻⁴ s⁻¹ to yield only **15** by C−OMe cleavage.[18,51] Additionally, the slow cleavage of DMPF (k_{obs} = 7.6 × 10⁻⁷ s⁻¹ at pH 8.4) by cetyltrimethylammonium iodosobenzoate also occurs with only C−OMe cleavage.[52] However, the scission of **8**, as might be expected, occurs with 90:10 P−OPh/C−OMe cleavage.[52]

25   **26**

Key:
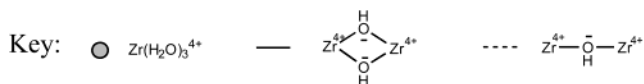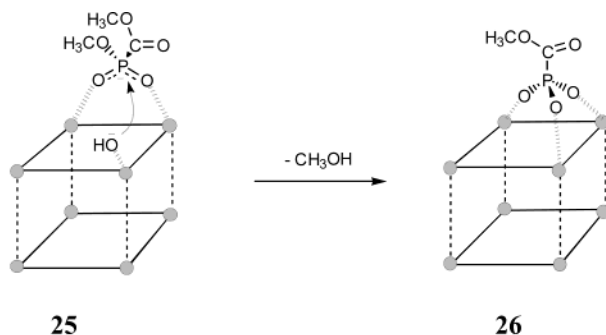
B. What Evidence Opposes These Models? Although the foregoing models rationalize the M(IV)-specific chemoselectivity and are consistent with the speciation studies, they are
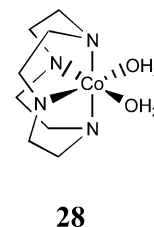
(48) Clearfield, A. *J. Mater. Res.* **1990**, *5*, 161.
(49) With substrate **8**, where P−O scission is advantaged by a phenoxide leaving group, these complexes afford P−O/C−O cleavage ratios of 1.1−1.3.[43]
(50) Chin, J.; Banaszczyk, M.; Jubian, V.; Zou, X. *J. Am. Chem. Soc.* **1989**, *111*, 186.
(51) Analogous results with other Co complexes are presented in Morales-Rojas, H. Ph.D. dissertation, Rutgers University, 2001.
(52) Moss, R. A.; Vijayaraghavan, S.; Kanamathareddy, S. *Langmuir* **2002**, *18*, 2468.

not in straightforward accord with the kinetic data as expressed in the correlations of log k_{obs} vs log[M(IV)]. These determinations were carried out in both H₂O and D₂O for the cleavages of substrate **8** by Zr(IV) and substrate **9** by Th(IV). The slopes of the linear correlations for **8** with Zr(IV) were 0.84 (H₂O) and 0.79 (D₂O), and for **9** with Th(IV) they were 0.82 (H₂O) and 0.84 (D₂O).

In principle, the dependence of log k_{obs} on log[M(IV)] should give the reaction order in the metal ion if the kinetics followed the simple relation: $k_{obs} = k_2[M]_{total}$. However, the experimental dependences give slopes that are <1, indicating a more complex relation between k_{obs} and [M(IV)]. At face value, these results indicate that higher order complexes (dimers, tetramers) are not the major catalytic species involved in these reactions. If they were, we would expect an upward curvature in the k_{obs} vs [M(IV)] plot, and the log k_{obs} vs [M(IV)] plot should give a slope > 1.[53]

27
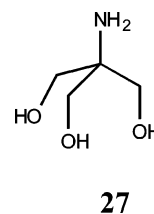
C. Can One Model the Observed Kinetics with Higher Order M(IV) Species? In an effort to link the possible contributions of different metal species to the dependence of k_{obs} on [M(IV)], we evaluated the equilibrium concentrations of Zr(IV) species within the concentration range studied (2.5− 25 mM), in water at pH 1.0 (see Table S1 in the Supporting Information and Figure 3). According to the calculated equilibrium concentrations, Zr tetramers and octamers are dominant under these conditions and together account for 92−98% of the total Zr(IV). If these species are the major contributors to the catalysis, the observed rate constant could follow a dependence like $k_{obs} = k_4[tetramer] + k_8[octamer]$. The equilibrium concentrations of Zr(IV) tetramers and octamers as a function of the total concentration of Zr(IV) (see Figure S5 in the Supporting Information) do not curve upward, and the log− log correlations of k_{obs} for the cleavage of **8** with the concentrations of Zr tetramers or octamers are linear, with slopes of 1.38 and 0.69, respectively (see Figure S6 in the Supporting Information).

28

Multiple regression analysis of the observed rate constants, fit to the equation $k_{obs} = k_4[tetramer] + k_8[octamer]$, afforded second-order rate constants $k_4 = 6.92 \pm 1.4$ and $k_8 = 5.47 \pm 0.59$ M⁻¹ s⁻¹, with $R^2 = 0.996$. The theoretical fit of the experimental k_{obs} using these parameters and the equilibrium concentrations of tetramers and octamers is remarkably good, as shown in Figure S7 (Supporting Information). The calculated

rate constants for the Zr(IV) tetramers and octamers are nearly equal, indicating similar reactivity of each species toward substrate **8**, in agreement with the model proposed in **25** and **26**.

The foregoing results indicate that the observed rate constant does not correlate with the concentration of a single Zr(IV) species but follows a more complex dependence that can be modeled in a linear fashion by the contributions of two higher order Zr complexes as shown in Figure S7. This does not exclude the intervention of still other Zr species, but it is of interest that the model predicts the observed linear behavior of k_{obs} and [Zr(IV)]$_{total}$. Linear correlations of k_{obs} vs total metal concentration have also been found in the cleavage of phosphate diesters by dinuclear lanthanide species.[54]

Conclusions

Ce(IV), Th(IV), Zr(IV), and Hf(IV) cations markedly accelerate the hydrolyses of phosphonoformate diester substrates **7**−**10**. Most importantly, our studies on the metal-mediated cleavages of these bifunctional esters illuminate a feature not previously associated with "bare" tetravalent metal salts in aqueous solutions: *chemoselective ester hydrolysis*. Unprecedented chemoselectivity is displayed in these reactions, whereby Zr and Hf direct scission at the P−O ester site, while Ce and Th activate the C−O ester site. Leaving group efficacy modulates the chemoselectivity: with substrate **9**, C−OPh cleavage dominates P−OMe cleavage even with Zr(IV) and Hf-(IV) catalysts, although the innate P−O selectivity of these cations is sufficiently robust to impose some competitive P−OMe cleavage, even in this biased case.

We consider a model in which the P−O selectivity of Zr-(IV) and Hf(IV) toward phosphonoformate diesters is linked to the presence of octameric/tetrameric complexes of the cations and can be shifted toward C−O selectivity by modification of the complexes, whereas C−O esterolytic selectivity is associated with dinuclear or mononuclear species of, e.g., Ce(IV), Th(IV), Co(III), Eu(III), or La(III). Binding of the substrate (Lewis acid activation) and reaction with a metal-coordinated water or hydroxide nucleophile account for both the observed reactivity and chemoselectivity. However, the kinetic dependences of the metal-ion-mediated cleavages on [M(IV)]$_{total}$ are not in full agreement with higher order metal complexes as the major catalytic entities. Therefore, the proffered models should not be regarded as established, but there is no gainsaying the unprecedented, clearly expressed, chemoselective proclivities of the several metal cations toward the phosphonoformate diester substrates.

Experimental Section

General Methods. Routine ^{1}H NMR spectra were determined at 300 or 400 MHz. ^{31}P NMR spectra were obtained at 121.4 or 161.9 MHz. ^{13}C NMR spectra were obtained at 100.6 MHz. Chemical shifts are reported as ppm (δ) relative to TMS or DSS for ^{1}H, external H$_3$-PO$_4$ (85%) for ^{31}P, or dioxane (67.4 ppm) for [13]C. UV−vis kinetics studies were obtained with a Hewlett-Packard 8453A diode array spectrophotometer with thermostated cells. pH measurements were made with an Orion 7110SC electrode, referenced with standard buffer

solutions. For deuterated aqueous solutions, pD was calculated according to the following equation: pD = pH meter reading + 0.40.[55] Melting points are uncorrected. Microanalyses were performed by Quantitative Technologies, Inc., Whitehouse, NJ.

Materials. Zirconium tetrachloride anhydrous (ZrCl$_4$), zirconium oxychloride hydrate (ZrOCl$_2$·8H$_2$O), hafnium tetrachloride anhydrous (HfCl$_4$), ceric ammonium nitrate (Ce(NH$_4$)$_2$(NO$_3$)$_6$), and thorium nitrate hydrate (Th(NO$_3$)$_4$·H$_2$O) were purchased from Strem Chemicals. Trimethyl phosphonoformate, phenyl chloroformate, trimethyl phosphite, trimethylsilyl bromide, phosphorus pentachloride, 1,8-diazabicyclo-[5.4.0]undecane (DBU), and phenol were purchased from Aldrich Chemical Co.. Phosphonoformate trisodium salt was purchased from ICN Chemicals. 1,4,7-Triazacyclononane(3HCl) was purchased from TCI America.

Deutereated solvents (D$_2$O, CDCl$_3$) and MeOH (99% [13]C) were obtained from Cambridge Isotope Laboratories. H$_2$[18]O with 43.85% or 85% of enrichment was obtained from ICON Laboratories. Anhydrous THF and DMF were used as supplied from Aldrich. All other solvents and salts were analytical grade unless otherwise stated.

Substrates. A. Dimethyl Phosphonoformate (7). To a solution of trimethyl phosphonoformate (2.5 g, 14.9 mmol) in acetone (30 mL) was added a solution of sodium iodide (2.23 g, 14.9 mmol) in acetone (30 mL).[4,56] The reaction mixture was stirred and heated under reflux for 2 h. Diester **7** was precipitated as a white solid. After filtration, the solid was washed with cold acetone and dried under vacuum to give 2.1 g of the sodium salt (80% yield); mp 179−181 °C (lit. 183 °C).[57]

^{1}H NMR (D$_2$O): 3.71 (s, 3H), 3.58 (*d*, 3H, J_{P-H} = 11.1 Hz). ^{31}P NMR (D$_2$O):[19] −2.6 (s, H-decoupled; q H-coupled). Anal. Calcd for C$_3$H$_6$O$_5$PNa: C, 20.5; H, 3.4. Found: C, 20.5; H, 3.2.

B. Methoxycarbonyl Phenylphosphonate (8). Following the method of McKenna,[58] trimethylsilylbromide (22.5 g, 14.7 mmol) was added with stirring to trimethyl phosphonoformate (12.5 g, 7.14 mmol), under N$_2$, previously cooled in an ice water bath; see Scheme 1. After addition was complete, the reaction mixture was allowed to warm to room temperature. After removal of methyl bromide under vacuum, the sample was purified by distillation under reduced pressure (54 °C, P < 0.01 mmHg) to give 18.5 g of colorless liquid bis-trimethylsilyl-(methoxycarbonyl) phosphonate **11** (91%). ^{31}P NMR (CDCl$_3$): δ −25.1.

Next, 18.5 g (6.5 mmol) of this liquid was dissolved in 50 mL of CH$_2$Cl$_2$ and added dropwise to a solution of PCl$_5$ (29 g, 13.1 mmol) suspended in 50 mL of CH$_2$Cl$_2$ under N$_2$, previously cooled to 0 °C. The reaction mixture was stirred at room temperature for an additional 4 h. The volatiles were evaporated, and the final liquid was distilled under reduced pressure (35 °C, P < 0.01 mmHg) to give 8 g of colorless liquid methoxycarbonyl phosphonodichloridate **12** (69%); ^{31}P NMR (CDCl$_3$): δ 9.8.

To a solution of methoxycarbonyl phosphonodichloridate (300 mg, 1.75 mmol) in 15 mL of dry CH$_2$Cl$_2$ under N$_2$, previously cooled to 0 °C, was added dropwise a solution of phenol (330 mg, 3.5 mmol) and DBU (0.53 g, 3.5 mmol) in 15 mL of dry CH$_2$Cl$_2$. The mixture was allowed to warm and stir for an additional 2 h. The organic phase was extracted twice with aqueous NaHCO$_3$ solution (0.06 g/50 mL) and then washed with 50 mL of water. The organic phase was dried over Na$_2$SO$_4$ and evaporated under vacuum to give a liquid containing methoxycarbonyl diphenylphosphonate **13** as the major component (68%, ^{31}P NMR CDCl$_3$, δ −15.3, s). The liquid was redissolved in 15 mL of CH$_3$CN and 20 mL of a NaHCO$_3$ solution (0.088 g) was added. The mixture was stirred at room temperature for 3 h. Acetonitrile was removed in a vacuum, and the aqueous solution was extracted with (2 × 30 mL) of CH$_2$Cl$_2$. The aqueous phase was lyophilized to give solid **8**, 0.25 g (60% yield); mp 80−82 °C (lit. 79−81 °C).[4]

(53) (a) Wahnon, D.; Hynes, R. C.; Chin, J. *Chem. Commun.* **1994**, 1441. (b) Jurek, P. E.; Jurek, A. M.; Martell, A. E. *Inorg. Chem.* **2000**, *39*, 1016.
(54) Gomez-Tagle, P.; Yatsimirsky, A. K. *Inorg. Chem.* **2001**, *40*, 3786.

(55) Glasoe, P. K.; Long, F. A. *J. Phys. Chem.* **1960**, *64*, 188.
(56) Zervas, L.; Dilaris, I. *J. Am. Chem. Soc.* **1955**, *77*, 5354.
(57) U.S. Patent 4018854; *Chem. Abstr.* CAN 87: 135910.
(58) McKenna, C. E.; Higa, M. T.; Cheung, N. H.; McKenna, M.-C. *Tetrahedron Lett.* **1977**, 155.

^{1}H NMR (D$_2$O): 7.09−7.33 (m, 5H), 3.74 (s, 3H). ^{31}P NMR (D$_2$O) −7.4 (s, H-decoupled). Anal. Calcd for C$_8$H$_8$O$_5$PNa: C, 40.3; H, 3.38. Found: C, 40.2; H, 3.41.

C. Phenoxycarbonyl Methylphosphonate (9). Trimethyl phosphite (10.5 g, 0.08 mol) was added dropwise over a period of 30 min with stirring to phenylchloroformate (12.6 g, 0.08 mol), under N$_2$, and previously cooled in an ice−water bath. After addition was complete the mixture was allowed to warm and stir for an additional 3 h. Volatiles were removed under vacuum to give 18 g (97%) of colorless liquid phenoxycarbonyl dimethylphosphonate. No further purification was performed on this product. ^{31}P NMR (CDCl$_3$): δ −4.72 (s proton decoupled; septet proton coupled). ^{1}H NMR (CDCl$_3$): δ 7.37 (t, 2H), 7.24 (t, 1H), 7.12 (d, 2H), 3.98 (d, 3H, J_{P-H} = 11.4 Hz).

To a solution of phenoxycarbonyl dimethylphosphonate (3.45 g, 15 mmol) in 30 mL of acetone under N$_2$ was added a solution of sodium iodide[4,56] (2.25 g, 15 mmol) in 30 mL of acetone. The reaction mixture was stirred and heated under reflux for 3 h. The solvent was removed to give a sticky solid, which was dissolved in acetone. Upon addition of ethyl ether, and after standing for 2 h, a white solid precipitated. The solid was filtered and dried under vacuum to give the sodium salt of diester **9** (2.85 g, 80% yield); mp 220−222 °C.

^{1}H NMR (D$_2$O): 7:12−7.43 (m, 5H), 3.72 (d, 3H, J_{P-H} = 10.8 Hz). ^{31}P NMR (D$_2$O): −3.26 (s, H-decoupled). Anal. Calcd for C$_8$H$_8$O$_5$ PNa: C, 40.3; H, 3.38. Found: C, 40.0; H, 3.30.

D. Diphenyl Phosphonoformate (10). Diphenyl phosphite (1.5 g, 5.68 mmol) was dissolved in 75 mL of dry, distilled THF in a 250-mL round-bottom flask, cooled in an ice−salt bath. Then, 0.32 g of a 60% NaH dispersion in mineral oil (7.85 mmol) was added. The contents were stirred at 0 °C for about 3 h. Then, 2.2 g (14 mmol) of phenylchloroformate in 5 mL of THF was added dropwise to the flask. After the addition, the contents were allowed to warm to room temperature and stirred for about 24 h. THF was removed on a rotary evaporator. About 15 mL of cold H$_2$O was added to the flask to decompose excess NaH, and the aqueous layer was extracted with 2 × 40 mL of methylene chloride. The organic layer and the extract were combined and dried over NaSO$_4$ and then evaporated to give crude triphenyl phosphonoformate triester (3.0 g) as a colorless liquid. The crude ester (0.75 g) was not purified and was directly hydrolyzed with 150 mg of NaHCO$_3$ in a 5 mL of H$_2$O/5 mL of CH$_3$CN mixture with stirring at room temperature for about 4 h. (Longer times or an excess of NaHCO$_3$ led to further decomposition.) After the reaction, the acetonitrile and most of the water were removed by rotary evaporation, and the crude residue was washed with ether. At this point, a white solid product precipitated. It was filtered, dried, and column-chromatographed after adsorption onto silica gel and eluted with 10% MeOH/ 90% EtOAc to give ∼100 mg of the purified sodium diphenyl phosphonoformate (**10**) as a white solid, mp 366−368 °C.

^{1}H NMR (D$_2$O): 7.00−7.40 (m). ^{31}P NMR (D$_2$O) − 8.23. ^{13}C NMR (D$_2$O): 121, 122, 125, 128, 130. Anal. Calcd for C$_{13}$H$_{10}$O$_5$PNa· 0.5H$_2$O: C, 50.5; H, 3.26; P, 10.0. Found: C, 50.6, H, 3.61; P, 10.0.

Intermediates.[59] A. Disodium Methoxycarbonyl Phosphonate (14). Bis-trimethylsilyl methoxycarbonyl phosphonate [**11**, see above and Scheme 1] (2 g, 7 mmol) in 30 mL of ether was extracted with 2 × 30 mL of a solution of 1.14 g of NaHCO$_3$ in 60 mL of water. Strong CO$_2$ evolution occurred and left a neutral aqueous solution from which lyophilization gave white solid **14**; mp > 300 °C.

^{1}H NMR (D$_2$O): 3.6 (s). ^{31}P NMR (D$_2$O): −5.2.

B. O-Methyl disodium oxycarbonyl phosphonate (15) was prepared by the hydrolysis of DMPF (**7**) with 1 equiv of NaOH solution. Lyophilization of the aqueous solution gave a white solid; mp > 300 °C.

^{1}H NMR (D$_2$O): 3.49 (d, J_{P-H} = 10.8 Hz). ^{31}P NMR (D$_2$O): 3.3 (s, H-decoupled).

C. O-Phenyl disodium oxycarbonyl phosphonate (18) was prepared by the hydrolysis of **8** with 1 equiv of NaOH solution. Lyophilization of the aqueous solution gave a white solid; mp > 300 °C.

^{1}H NMR (D$_2$O): 7.0−7.3 (m). ^{31}P NMR (D$_2$O) 4.2.[19]

D. Disodium phenoxycarbonyl phosphonate (20) was prepared from bis-trimethylsilyl phenoxycarbonyl phosphonate in a fashion similar to that for **14**; mp > 300 °C.

^{1}H NMR (D$_2$O): 7.09−7.41 (m). ^{31}P NMR (D$_2$O): −3.2.[19]

Kinetics. Data for substrates **7**, **8**, **9**, **14**, and **15** were obtained by NMR monitoring of the corresponding released alcohol fragment, MeOD. Kinetics data were also obtained from the disappearance of the substrate if its signal was resolved enough to give accurate integrals. For rapid kinetics, 40 μL of a 0.5 M substrate stock solution was added to 2 mL of a 0.025 M M(IV) solution containing 2.5 × 10^{-3} M of pyrazine (integration standard) and 0.5 M NaClO$_4$. The pD of the M(IV)−pyrazine−NaClO$_4$ solution was established by the natural hydrolysis of the metal salt under these conditions. No DCl or NaOD was added unless otherwise noted. The vial was shaken to ensure homogeneity, and 700 μL were quickly transferred to a 5 mm NMR tube. After loading, equilibrating and tuning the NMR spectrometer at 25 °C (∼3 min), we acquired the spectra at preset time intervals. In a typical experiment, the parameters were 1.6 s acquisition time, 1.0 s delay, 5000 Hz sweep width, 16 K data block, and 32 accumulated transients. For control experiments, the reaction mixtures were prepared as described above. The pH value was adjusted with 1 N DCl. The NMR tube was incubated in a water bath at 25 °C. At suitable time intervals, the tube was removed and NMR spectra were collected.

Kinetics were followed up to 5 half-lives, 25 to 40 points were taken, and the endpoint (I_∞) was obtained after 10 half-times. The raw integrals obtained in each spectrum were normalized by dividing by the integral of the pyrazine standard. The pseudo-first-order rate constants were calculated by plotting ln($I_\infty − I_t$) vs time for the released species or ln(I_t) vs time for the disappearance of substrates. Rate constants are the averages of duplicate runs.

Kinetics for the cleavage of substrates **8**−**10**, **18**, and **20** were monitored by UV spectroscopy following the appearance of the released phenol at 260, 270, and 280 nm. In a typical experiment, 50 μL of a 12.5 mM stock solution of the substrate was added to 3 mL of 25 mM metal(IV) solution containing 0.5 M NaClO$_4$ in D$_2$O (or H$_2$O). Clean pseudo-first-order profiles were obtained over 5 half-lives. Rate constants are the averages of duplicate runs.

Product Studies by ^{31}P NMR. For these studies, 80 μL of a 0.5 M stock solution of substrates **7**−**9**, **14**, **15**, **18**, or **20** were added to 4 mL of a solution of 0.025 M M(IV) and 0.5 M NaClO$_4$ in D$_2$O. After shaking to ensure homogeneity, each vial was incubated at 25 °C. Aliquots (1 mL) were taken from the reaction mixture at different time intervals, and 35 mg of EDTA disodium salt was added. A solid precipitated right after the addition. After standing for 1−2 h at room temperature, the mixture became homogeneous and colorless. For substrates **8**, **18**, and **20**, in the presence of Th(IV), the solutions were quenched with 50 mg of tartrate disodium salt instead of EDTA.

Next, 700 μL of each of the above solutions (pH 3.5) were transferred to 5-mm NMR tubes. After careful tuning and shimming of the NMR spectrometer, the proton coupled and decoupled ^{31}P NMR spectra were acquired at 25 °C, referenced to external 85% H$_3$PO$_4$. In a typical case the following parameters were used: 1.6 s acquisition time, 8000 Hz sweep width centered at −1100 Hz, 32 K data block, 1.0 s recycle delay, and 800 accumulated transients. Product identification was performed by the additions of small aliquots of authentic materials.

For substrate **10**, a 5-mL solution containing 25 mM metal ion [Zr-(IV) or Th(IV)] and 0.5 M NaClO$_4$, in 50% D$_2$O−50% CD$_3$CN, was prepared and thermostated at 25 °C. The solution was allowed to reach its pH by natural hydrolysis. To this was then added 100 μL of a

---

(59) Reaction intermediates are characterized spectroscopically; elemental analyses were not attempted. Note that the chemical shifts are somewhat different in the absence of M^{4+}. However, the various "synthetic" intermediates were identical to the corresponding "reaction" intermediates in NMR spiking experiments.

solution of 0.5 M substrate **10** (or **7**) in D_2O. Reactions were quenched at preset time intervals by removing 700-μL aliquots from the reaction mixture and adding ~20 mg of sodium tartrate. The solution was then transferred to a 5-mm NMR tube, and the ^{31}P NMR spectrum was determined at 25 °C in the presence of 2mM *O*-methyl methyl phosphonate (MMP) as an internal integration standard. In a typical NMR experiment, about 1500 transients (scans) were performed, and 32 000 data points were collected, with an acquisition time of 1.6 s.

Supporting Information Available: Figures of k_{obs} vs [M(IV)] and log k_{obs} vs log[M(IV)] for substrate **8** with Zr(IV) and substrate **9** with Th(IV); calculated equilibrium concentrations and rate constants for Zr(IV) tetramers and octamers in the cleavage of **8**. This material is available free of charge via the Internet at http://pubs.acs.org.

JA030437H